DESIGN AND SIMULATION ANALYSIS OF KEY COMPONENTS OF GRASS CRUSHER /
牧草粉碎机关键部件设计与仿真分析

Tao CHEN[1)], Shu-juan YI[*1)], Song WANG[1)], Wen-sheng SUN[1)]
[1)]College of Engineering, Heilongjiang Bayi Agricultural University, Daqing/P.R.China
Tel: +86-459-13836961877; E-mail: yishujuan_2005@126.com
Corresponding author: Shu-juan YI
DOI: https://doi.org/10.35633/inmateh-75-48

Keywords: *Pasture; Grinding machine; Design; Simulation analysis*

ABSTRACT
In view of the problems of low efficiency, poor crushing quality and inapplicability to high water content forage, the cutter and crusher rotor of hammer type forage grinder was designed, the cutter and crusher process was analyzed theoretically, and the parameters of cutter and crusher rotor were determined. The modal analysis of the cutting and crushing rotor was carried out by ANSYS Workbench, to verify the rationality of the rotor structure. The alfalfa with water content of 65% was taken as the processing object, and the quadratic orthogonal rotation combination test was carried out with the output speed of motor, sieve diameter and feeding amount as the test factors, and the productivity and silking rate as the evaluation indexes. Through the analysis of variance and target optimization of the test results by Design-Expert 12.0 software, the regression equation between the test factors and the evaluation index was obtained. With the goal of maximizing the productivity and silking rate at the same time, the output speed of the motor, the diameter of the sieve and the feeding amount were solved by multi-objective optimization, and the optimal parameter combination was determined as follows: the output speed of the motor is 443.77r/min, the diameter of the sieve is 14mm, and the feeding amount is 1.27kg/s. The verification test shows that the productivity is 5065.98 kg/h, and the silk rates is 94.87%. The device has high crushing efficiency, good quality, and can crush high water content forage, which meets the design requirements of forage mill.

摘要
针对现有的牧草粉碎机效率低、粉碎质量差、对高含水率牧草不适用等问题，对锤片式牧草粉碎机的铡切和粉碎转子进行了创新设计，对铡切和粉碎过程进行了理论分析，确定了铡切和粉碎转子的参数。利用 ANSYS Workbench 对铡切和粉碎转子进行了模态分析，验证转子结构的合理性。将含水率为65%的苜蓿作为加工对象，进行了以电机输出转速、筛孔直径、喂入量为试验因素，以生产率和丝化率为评价指标的二次正交旋转组合试验。通过 Design-Expert 12.0 软件对试验结果进行了方差分析及目标优化，得到了试验因素与评价指标之间的回归方程，以生产率和丝化率同时最大化为目标，对电机输出转速、筛孔直径、喂入量进行多目标寻优求解，确定最优参数组合为：电机输出转速 443.77r/min、筛孔直径 14mm、喂入量 1.27kg/s，验证试验表明，生产率为 5065.98kg/h、丝化率为 94.87%；该装置粉碎效率高、质量好，而且能够粉碎高含水率牧草，满足牧草粉碎机设计要求。

INTRODUCTION
As one of the important links of grass processing, crushing quality has an important impact on processing cost and livestock digestion effect (*Wu et al., 2022; Wang et al., 2017*). Crushing is to cut off the grass and expose its internal nutrients, which can not only improve palatability, but also increase the contact area with the stomach juice of livestock, shorten the rumination and chewing time, and reduce the energy consumed by the chewing of livestock. The crushed grass is easy to chew and has a good taste, which promotes the absorption of nutrients by livestock (*Fang et al., 2021; Huan et al., 2021*). The length of forage required by ruminants is 30~50mm, and crushing too long or too short is not conducive to digestion and absorption. In order to prevent too short after stirring cutting, the length of the crushed grass should be 50~70mm *(Fan et al., 2021; Zheng et al., 2016; Li et al., 2019*).

[1]*Tao Chen, Ph.D.; Shu-juan Yi, Prof. Ph.D.; Song Wang, Ph.D.; Wen-sheng Sun, Ph.D.;*

Grass processing can be divided into shredding processing, crushing processing and kneading processing according to the crushing form, and the corresponding models are guilloff type mill, hammer type mill, kneading type mill, etc. (*Zhang et al., 2024; Liu et al., 2019*). The cut type crusher breaks the grass by cutting, although it has the advantages of simple structure, low power consumption and high productivity, but the processed broken grass is mostly round rod, and there are hard joints, which will lead to indigestion and palatability of livestock, which is not conducive to digestion and absorption of livestock (*Jiang et al., 2019*). Hammer mill first crushed the grass to a certain extent through the impact of the hammer, and then the grass was thrown to the kneading board and sieve plate at a faster speed in the crushing room, which was further crushed by the collision of the kneading board and the rubbing of the sieve plate. The crushing efficiency was high and the adaptability was wide, but the crushed grass was too fine, which could not make its fiber better retained. As a result, it has a low volume and cannot be stored for a long time (*Liu et al., 2011*). Under the kneading action of the high-speed rotating hammer and tooth plate, the crushed grass is broken into soft and fluffy filamentous segments, exposing nutrients, increasing the contact area with the digestive system of livestock, and promoting digestion and absorption (*Ma et al., 2016*).

In terms of forage processing machinery, foreign countries have complete types, relatively perfect functions and mature technologies, but they are mainly used in large-scale farmland and pasture, and are not suitable for the miniaturization and convenience of forage processing machinery in small-scale breeding areas in China. Domestic scholars have been committed to the research of grass processing machinery, more and more new models continue to emerge. *Wang Defu et al*., *(2017),* used high-speed camera technology to analyze the crushing mechanism of the hammer mill, and conducted experimental research on crushing performance. They found that the crushing forms of the hammer mill were mainly percussion crushing, impact crushing and rubbing crushing, and the impact crushing and rubbing crushing had a greater impact in the crushing process. It is concluded that the linear speed of the end of the hammer and the water content of the material have great influence on the crushing effect of the hammer mill. *Wang Tiejun et al. (2021*), designed a feeding-adjustable straw breaking and kneading machine to solve the problem that the existing machine could not adapt to the whole bundle manually packed and the small square bundle mechanically pressed corn straw simultaneously. Through the analysis of the force and movement of straw in each device of the machine, the key structure of the whole machine is designed and matched with the drive system, and the kneading performance test is carried out to realize the localized kneading treatment of scattered bale straw in the village. *You Yong et al. (2021*) designed a 4-row herringbone roller crushing device based on the agronomic requirements of king grass harvester crushing, combined with the characteristics of strong tillering ability, large biomass and high-water content of king grass. The main structure and parameters of the crushing device are determined by theoretical analysis and calculation. The test shows that the length of the king grass broken by the device is uniform and the qualified rate of the stalk broken is high, which can meet the requirements of the king grass broken during the harvest period. Although after years of painstaking research by many scholars, the kneading quality of forage grass has been improved to a certain length, due to the strong toughness of forage grass with high moisture content, the force required when it is broken by blows and other effects is greater, and the whole forage grass is easy to wrap around the rotor when it is crushed, causing blockage. Therefore, the existing grinding machine still has some problems, such as low efficiency, poor kneading quality, and not suitable for forage with large moisture content.

In this paper, taking alfalfa as the processing object, the cutting and crushing rotors of hammer forage crusher are innovated. The forage is cut before it is crushed, and it is cut into small segments of certain length by means of cutting rotor. Thus, the crushing quality and production efficiency can be improved, and the high-water content forage can be crushed.

MATERIALS AND METHODS

Structure and working principle

The cutting and crushing combined grass crusher is mainly composed of motor, frame, conveying mechanism, feeding mechanism, cutting mechanism, crushing mechanism, screening mechanism, transmission system and other parts. The structure is shown in Fig.1.

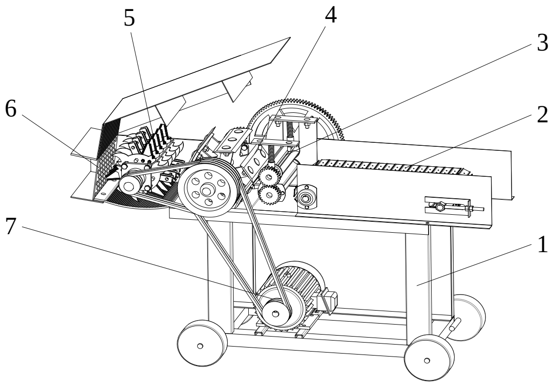

Fig.1 - Structure diagram of cutting and crushing cooperative grass crusher

1. Frame; 2. Conveying mechanism; 3. Feeding mechanism; 4. Cutting mechanism;
5. Crushing mechanism; 6. Sieve plate; 7. Motor

During operation, the whole grass is transported to the feeding mechanism through the conveying mechanism, and the feeding mechanism evenly feeds the grass into the cutting room to complete the feeding. The cutting mechanism breaks the grass into small segments of a certain length to complete the cutting. The crushing mechanism breaks the cut grass into filaments and completes the crushing. The crushed grass that meets the crushing length is thrown to the outside of the body through the screen plate through the dual action of the air flow generated by the rotation of the crushing rotor and the centrifugal force to complete the screening and throwing.

Force analysis and mechanism design of alfalfa during cutting process

The force analysis of alfalfa during cutting process is shown in Fig.2.

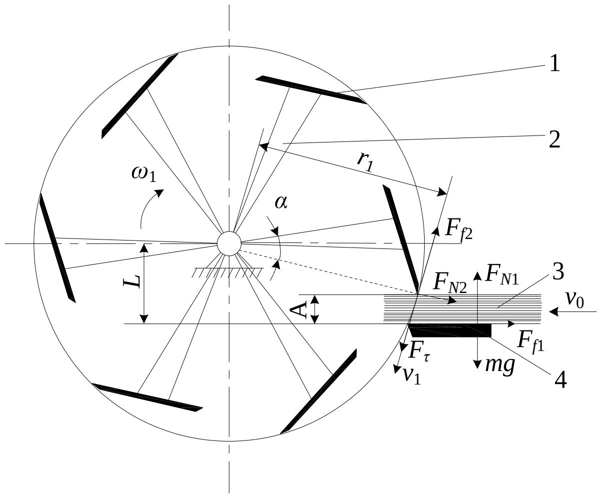

Fig. 2 - Analysis of the force and motion of alfalfa during the cutting process

1. Moving cutter; 2. Knife holder; 3. Alfalfa; 4. Fixed cutter

According to the cutting effect of moving and fixed knives on alfalfa, and the analysis of the force and movement of alfalfa in the process of cutting, the necessary conditions for cutting alfalfa are obtained:

$$F_\tau \sin\alpha \geq F_{f1} + F_{f2}\sin\alpha + F_{N2}\cos\alpha \tag{1}$$

It can be seen from Fig.2 that:

$$mg + F_\tau\cos\alpha + F_{N2}\sin\alpha = F_{N1} + F_{f2}\cos\alpha \tag{2}$$

$$F_{f1} = \mu_1 F_{N1} \tag{3}$$

$$F_{f2} = \mu_2 F_{N2} \tag{4}$$

where: α is the sliding cutting angle, (°); m is alfalfa mass, kg; g is acceleration of gravity, m/s^2; F_τ is the cutting force of cutter on alfalfa, N; F_{N1} is the supporting force of cutter on alfalfa, N; F_{N2} is the positive pressure of a cutter on alfalfa, N; F_{f1} is the friction of cutter against alfalfa, N; F_{f2} is cutter friction on alfalfa, N; μ_1 is the friction factor between alfalfa and moving cutter; μ_2 is the friction factor between alfalfa and fixed cutter.

In this study, the design of the moving cutter and fixed cutter use the same material, the alfalfa and their friction factors are the same, that is, $\mu_1=\mu_2=\mu$, the joint vertical (1) ~ (4) can be obtained:

$$\mu+\frac{F_{N2}\cos(2\alpha)+mg\sin\alpha}{F_{N1}\cos\alpha}\le\tan\alpha \tag{5}$$

$$\frac{F_{N2}\cos(2\alpha)+mg\sin\alpha}{F_{N1}\cos\alpha}\ge 0 \tag{6}$$

If formula (5) is established, the tangent value of alfalfa friction angle $\tan\varphi\le\tan\alpha$ can be obtained, and the friction angle of alfalfa is generally φ=24º~32º (*Chen et al., 2023*), that is, $\alpha \ge 32^{\circ}$.

In order to facilitate the balanced sliding of alfalfa and reduce power consumption, the cutter should be inclined to install, but the inclination angle is too large to affect the dynamic balance and vibration, so the sliding angle is designed to be 32º, the circumferential interval of 60º is arranged with 1 blade cutter, the cutter shaft is arranged with 6 blades, guilloff cutter structure is shown in Fig.3.

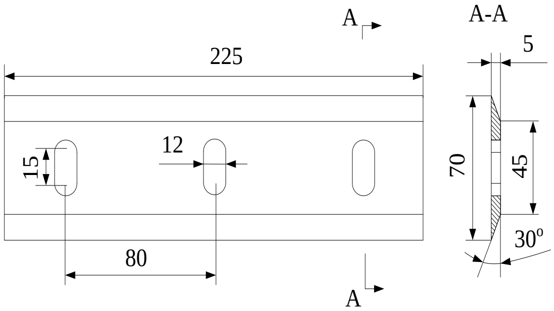

Fig. 3 - Structure diagram of the moving cutter

Force analysis and mechanism design of alfalfa in crushing process

The forces in alfalfa crushing process are shown in Fig.4.

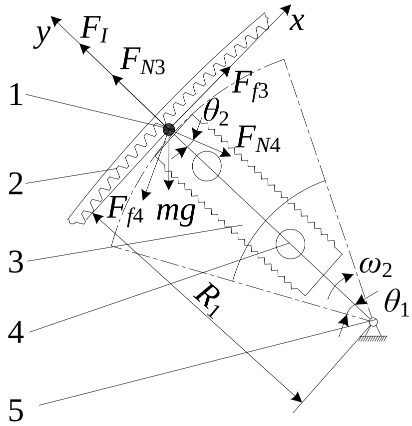

Fig. 4 - Stress Analysis of Alfalfa Silk Rolling Process

1. Alfalfa; 2. Kneading board; 3. Hammer; 4. Pin; 5. Crushing shaft

According to D 'Alembert's principle, alfalfa should meet the equilibrium state at the moment of crushing, and the equilibrium equation is established:

$$\begin{cases}\sum F_x = F_{f3}+F_{N4}\sin\theta_2 - F_{f4}\cos\theta_2 - mg\cos\theta_1 = 0\\ \sum F_y = F_I + F_{N3} - F_{N4}\cos\theta_2 - F_{f4}\sin\theta_2 - mg\sin\theta_1 = 0\end{cases} \tag{6}$$

$$F_I = m\omega_2^2 R_1 \tag{7}$$

$$F_{f3} = \mu_3 F_{N3} \tag{8}$$

$$F_{f4} = \mu_4 F_{N4} \tag{9}$$

Equations (6) ~ (9) can be obtained simultaneously:

$$\begin{cases} F_{f3} = mg\cos\theta_1 + \Big\{ \left[\mu_3 m\omega_2^2 R_1 + mg\left(\cos\theta_1 - \mu_3\sin\theta_1\right)\right]\cdot \\ \qquad \left(\mu_4\cos\theta_2 - \sin\theta_2\right)\left[\left(1+\mu_3\mu_4\right)\sin\theta_2 + \left(\mu_3 - \mu_4\right)\cos\theta_2\right]^{-1} \Big\} \\ F_{f4} = \mu_4 \dfrac{\mu_3 m\omega_2^2 R_1 + mg\left(\cos\theta_1 - \mu_3\sin\theta_1\right)}{\left(1+\mu_3\mu_4\right)\sin\theta_2 + \left(\mu_3-\mu_4\right)\cos\theta_2} \end{cases} \tag{10}$$

where:

ω_2 is the hammer angular velocity, rad/s; θ_1 - the horizontal angle between the alfalfa segment and the axis of the crushing shaft, (°); θ_2 - the angle between the alfalfa segment and the axis of the kneading shaft and the direction of the kneading board's supporting force on the alfalfa, (°); F_I - the centrifugal force in alfalfa section, N; F_{N3} - the supporting force of the hammer on alfalfa segment, N; F_{N4} - the support force of knead board on alfalfa segment, N; F_{f3} - the friction force of hammer against alfalfa segment, N; F_{f4} - friction force of kneading board on alfalfa segment, N; R_1 - alfalfa section turning radius, mm; μ_3 - friction factor between alfalfa segment and hammer piece; μ_4 - friction factor between alfalfa segment and kneading board.

Formula (10) shows that the friction force F_{f3} and F_{f4} during the grinding of alfalfa are related to the friction factor, position and angular velocity, etc. The trapezoidal teeth on the surface of the kneading plate near the hammer can increase the friction factor. The angular speed of the hammer is directly determined by the speed of the grinding shaft. When the machine power and transmission ratio are constant, the speed of the grinding shaft is mainly affected by the output speed of the motor. In order to clarify the influence of the output speed of the motor on the grinding effect of alfalfa, this paper optimizes it through experiments.

The hammer is designed as a rectangular zigzag shape, which increases the friction between the hammer and the material while striking and crushing the alfalfa, and can also produce better sliding and stabbing effects. The serrated knife is hexagonal, and the cutting edges on both sides of the knife are made into serrated edges to improve the strength and wear resistance of the blade. The structure of the hammer and serrated knife is shown in Fig.5.

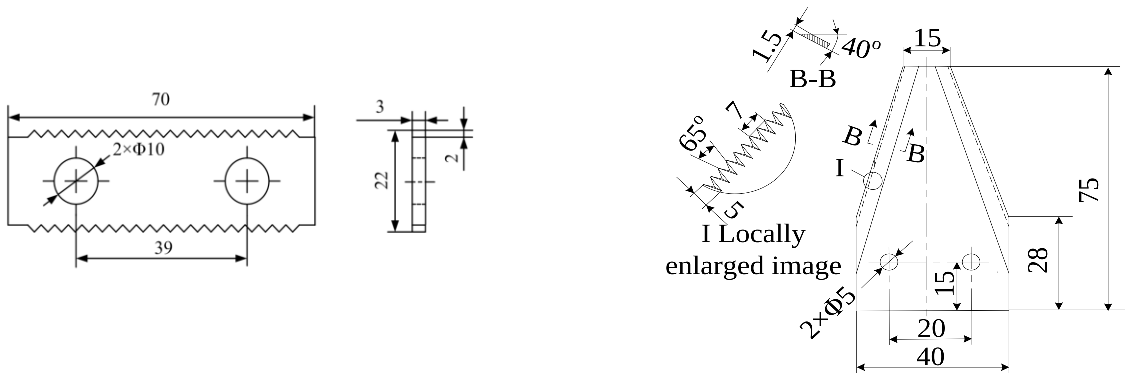

（a）Hammer （b）Serrated knife

Fig. 5 - Structure diagram of hammer and serrated knife

Modal analysis

ANSYS Workbench software is used to analyze the mode of the cutting rotor and crushing rotor of the grinder, analyze its vibration characteristics and deformation, and ensure its reliability in the working process.

The modal analysis results of the cutting rotor are shown in Table 1 and Fig. 6.

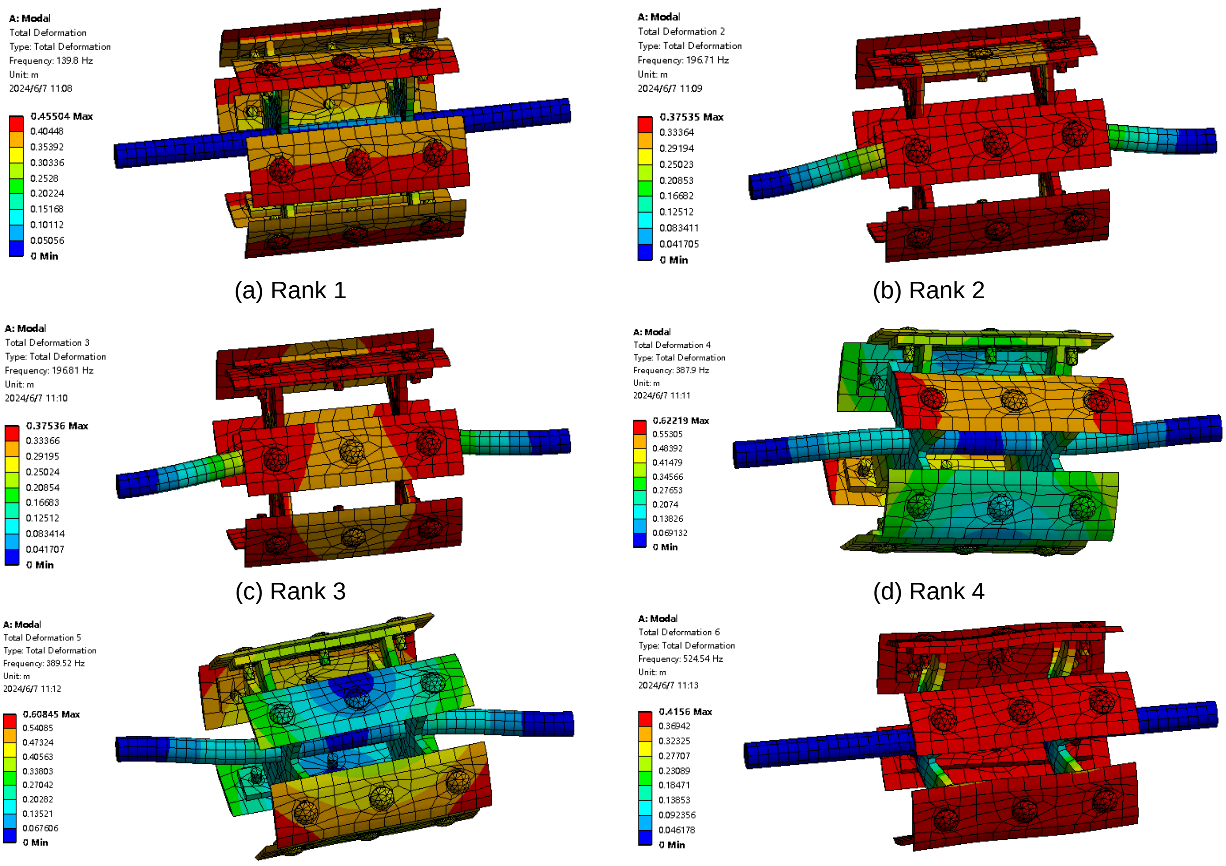

(a) Rank 1 (b) Rank 2

(c) Rank 3 (d) Rank 4

(e) Rank 5 (f) Rank 6

Fig. 6 - Cloud image of the first 6 modes of the cutting rotor

As can be seen from the Fig.6, the first-order vibration mode is represented by the deformation of the working edge surface of the cutter. The second order mode mainly shows the overall deformation of the rotor. The third order mode is mainly characterized by cutting tool deformation. The 4th-order mode mainly shows the deformation of cutting tool and tool holder. The 5th order mode is mainly tangential bending deformation. The 6th-order mode mainly shows the deformation of cutting tool and tool holder.

Table 1

Results of the first six modes of cutting rotor

Order	Intrinsic frequency/Hz	Maximum deformation/m	Main vibration mode
1	139.8	0.46	The working edge surface of the cutter is deformed
2	196.71	0.38	Integral rotor deformation
3	196.81	0.38	Cutter deformation
4	387.9	0.62	The cutter and tool holder are deformed
5	389.52	0.61	The cutting shaft is bent and deformed
6	524.54	0.42	The cutter and tool holder are deformed

In the process of rotor rotation, the excitation source mainly comes from self-rotation excitation. When the excitation frequency exceeds the natural frequency, the total performance of the rotor will have the risk of failure. The relation between the rotational speed of rotor and excitation frequency is

$$n = 60f \tag{11}$$

where: n is rotor assembly speed, r/min; f is rotary excitation frequency, Hz

The maximum working speed of the cutting rotor is 300r/min, and the maximum rotation excitation can be calculated to be 5Hz. Lower than the first order natural frequency 139.8Hz. Therefore, the designed cutter rotor can effectively avoid resonance phenomenon during high-speed rotation.

The modal analysis results of the crushed rotor are shown in Table 2 and Fig. 7.

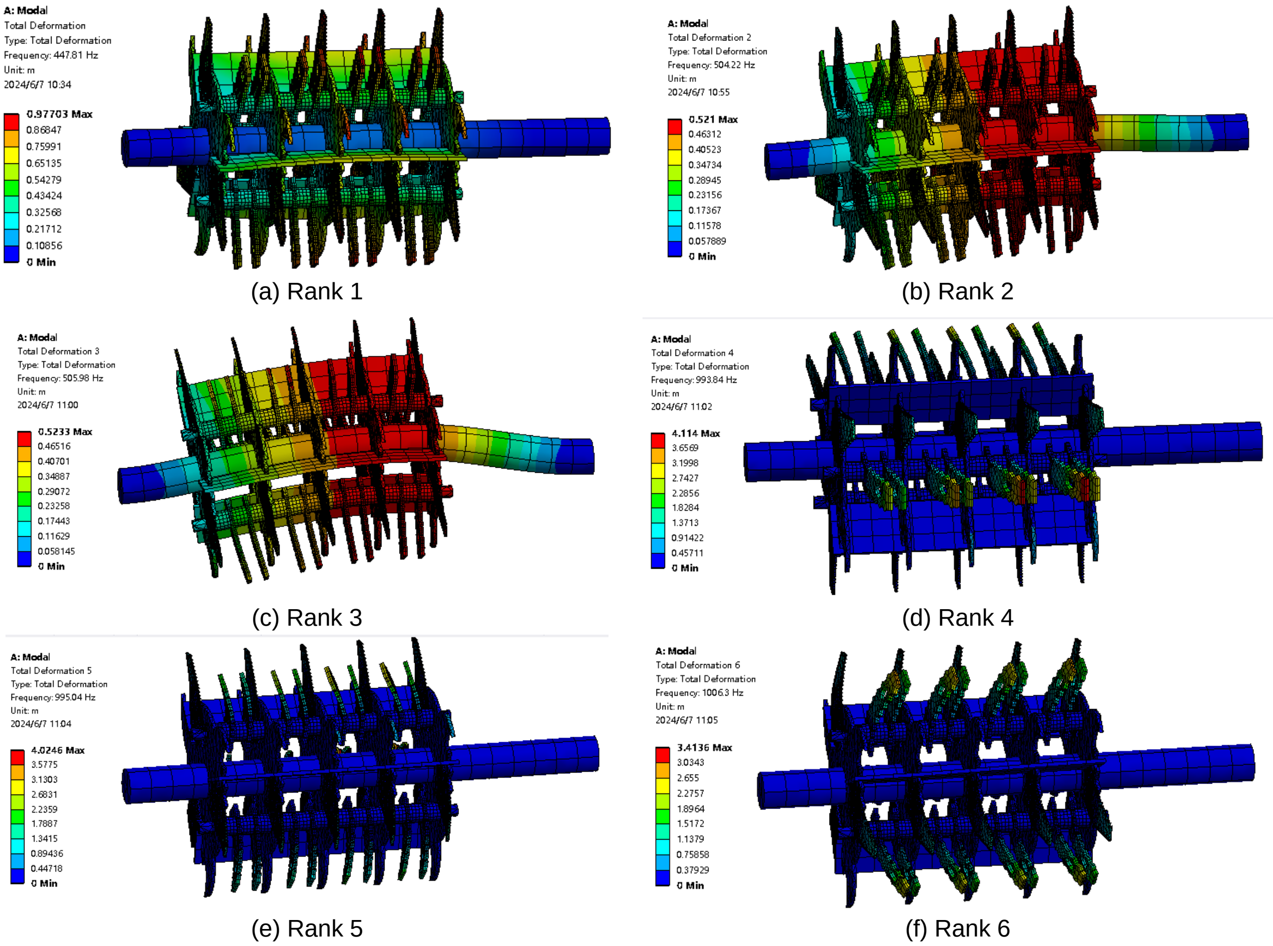

Fig. 7 - Cloud diagram of the first 6 orders of modal shapes of the crushing rotor

As can be seen from the Fig.7, the first-order vibration mode is manifested as the deformation of the outer edge of the hammer plate and the hammer frame plate. The second order mode mainly shows the deformation of rotor end and serrated knife. In the third order mode, the rotor is deformed as a whole. The fourth order vibration mode is mainly hammer deformation. The 5th order vibration mode is mainly hammer deformation. The 6-order vibration mode is mainly the hammer and serrated knife deformation.

Table 2

Results of the first 6 modes analysis of the crushed rotor

Order	Intrinsic frequency/Hz	Maximum deformation/m	Main vibration mode
1	447.81	0.97	The edge of the hammer plate and the hammer frame plate is deformed
2	504.22	0.52	The rotor end and serrated knife are deformed
3	505.98	0.52	Integral rotor deformation
4	993.84	4.11	Hammer deformation
5	995.04	4.02	Hammer deformation
6	1006.3	3.41	Hammer and serrated knife deformed

The maximum rotational speed designed for the grinding rotor is 800r/min, and the maximum rotational excitation calculated by formula (11) is 13.33Hz. Lower than the first order natural frequency 447.81Hz. Therefore, the designed grinding rotor can effectively avoid resonance during high-speed rotation.

RESULTS AND DISCUSSIONS

The design of the kneading machine prototype was made and the performance test was carried out. Alfalfa was processed and collected at the dry grass planting base in Duerbert County, Daqing City, Heilongjiang Province. The alfalfa collected was free of diseases, pests and obvious mechanical damage. The average moisture content of alfalfa was determined by random sampling to be 65%. The test was carried out in the crop harvest Laboratory of Heilongjiang Bayi Agricultural University, as shown in Fig.8.

Fig. 8 - Test bench for cutting and crushing cooperative silk kneading machine

1. Crusher; 2. Feed conveyor belt

Productivity y_1

The weighed straw was fed, the time required to crush all the straw was recorded, and the productivity y_1 was calculated as:

$$y_1 = \frac{m}{t} \times 3600 \tag{12}$$

where: m is quality of straw for test, kg; t is test time, s.

Silking rate y_2

Samples were collected at the outlet at the same time interval for 3 times, each time no less than 200g. All samples were mixed and weighed. Qualified alfalfa silk was screened and weighed, and the silking rate y_2 was calculated:

$$y_2 = \frac{m_2}{m_0} \times 100\% \tag{13}$$

where: m_2 is quanty of alfalfa silk in sample, g; m_0 is alfalfa sample quality, g

The code of test factors is shown in Table 3, and the test scheme and results are shown in Table 4.

Table 3

Factor level coding

Coding	Factor		
	Motor output speed x_1 (r/min)	The diameter of the screenx_2/mm	Feeding quantity x_2 (kg/s)
1.682	500	20	2.0
1	449.3（450）	18.8（19）	1.8
0	375	17	1.5
-1	300.7（300）	15.2（15）	1.2
-1.682	250	14	1.0

Table 4

Test scheme and results

Number	x_1	x_2	x_3	y_1/kg·h^{-1}	y_2/%
1	1	1	1	4590.21	95.84
2	1	1	-1	4365.4	94.62
3	1	-1	1	4952.07	94.53
4	1	-1	-1	4757.15	96.56
5	-1	1	1	4395.94	88.51
6	-1	1	-1	4513.76	92.68

Number	x_1	x_2	x_3	y_1/kg·h^{-1}	y_2/%
7	-1	-1	1	4582.55	83.41
8	-1	-1	-1	4588.32	91.62
9	1.682	0	0	4470.74	95.53
10	-1.682	0	0	4200.32	83.68
11	0	1.682	0	4390.6	93.87
12	0	-1.682	0	5149.43	93.35
13	0	0	1.682	5008.91	90.08
14	0	0	-1.682	4766.34	96.41
15	0	0	0	5137.16	91.63
16	0	0	0	5117.43	93.26
17	0	0	0	4974.76	91.85
18	0	0	0	5094.31	91.71
19	0	0	0	5070.22	91.64
20	0	0	0	5168.64	90.48
21	0	0	0	5171.6	90.15
22	0	0	0	5206.13	92.01
23	0	0	0	5095.08	92.23

The variance analysis results of the productivity and silk rate regression models were obtained, as shown in Table 5 and Table 6 respectively.

Table 5

Analysis of variance of productivity regression model

Source of variance	Sum of squares	Degree of freedom	Mean sum of squares	F	P
Model	2.24×10^6	9	2.49E+05	39.15	< 0.0001
x_1	79053.77	1	79053.77	12.44	0.0037
x_2	3.84×10^5	1	3.84×10^5	60.46	< 0.0001
x_3	36300.18	1	36300.18	5.71	0.0327
$x2$ 1	30312.14	1	30312.14	4.77	0.0479
$x2$ 2	36899.58	1	36899.58	5.81	0.0315
$x2$ 3	843.78	1	843.78	0.13	0.7215
x_1x_2	1.29×10^6	1	1.29×10^6	202.62	< 0.0001
x_1x_3	2.73×10^5	1	2.73×10^5	42.95	< 0.0001
x_2x_3	1.27×10^5	1	1.27×10^5	20.02	0.0006
Residual error	82629.68	13	6356.13		
Lack of fit	45249.84	5	9049.97	1.94	0.1936
Error	37379.83	8	4672.48		
Sum total	2.32×10^6	22			

Table 6

Analysis of variance for regression model of filamentization rate

Source of variance	Sum of squares	Degree of freedom	Mean sum of squares	F	P
Model	244.9	9	27.21	42.32	< 0.0001
x_1	149.99	1	149.99	233.27	< 0.0001
x_2	3	1	3	4.67	0.0499
x_3	41.6	1	41.6	64.7	< 0.0001
$x2$ 1	5.76	1	5.76	8.96	0.0104
$x2$ 2	16.73	1	16.73	26.02	0.0002
$x2$ 3	6.64	1	6.64	10.33	0.0068
x_1x_2	8.22	1	8.22	12.79	0.0034
x_1x_3	7.71	1	7.71	11.99	0.0042
x_2x_3	5.12	1	5.12	7.96	0.0144
Residual error	8.36	13	0.64		
Lack of fit	1.64	5	0.33	0.39	0.8426
Error	6.72	8	0.84		
Sum total	253.26	22			

As can be seen from Table 3, the productivity regression model (P=<0.0001) is significant, while the lack of fit (P=0.1936) is not, indicating that the model has a good degree of fitting and no misfit phenomenon occurs. The determination coefficient R2=0.9644, the correction determination coefficient Radj=0.9398, which is very close to 1, and the coefficient of variation is 1.66%, indicating that the test data is reliable. The predicted value of the regression equation has a significant relationship with the actual value obtained through the analysis of the test results. The regression equation of each factor and evaluation index obtained after removing the non-significant item is shown as follows:

$$\begin{aligned} y_1 &= 5115.98 + 76.08x_1 - 167.75x_2 + 51.56x_3 - 61.56x_1x_2 \\ &+ 67.92x_1x_3 - 10.27x_2x_3 - 284.7x_1^2 - 131.08x_2^2 \end{aligned} \tag{14}$$

According to Table 4, the silk rate regression model (P=<0.0001) was significant, while the lack of fit (P=0.8426) was not, indicating that the model had a good degree of fitting and no misfit phenomenon occurred. The determination coefficient R2=0.9670, the correction determination coefficient Radj=0.9441, which is very close to 1, and the coefficient of variation is 0.85%, indicating that the test data is reliable. The predicted value of the regression equation has a significant relationship with the actual value obtained through the analysis of the test results. The regression equation of each factor and evaluation index obtained after removing the non-significant item is shown as follows:

$$\begin{aligned} y_2 &= 93.66 + 3.31x_1 + 0.47x_2 - 1.75x_3 - 0.85x_1x_2 \\ &+ 1.45x_1x_3 + 0.91x_2x_3 - 0.72x_1^2 + 0.7x_2^2 + 0.57x_3^2 \end{aligned} \tag{15}$$

Parameter optimization and test verification

In order to obtain the optimal parameter combination of the operating performance of the kneading machine, the multi-objective optimization algorithm in the Design-Expert 12.0 software was used to establish an optimization mathematical model with the maximum productivity and maximum silking rate as optimization objectives, as shown in Equation (16).

$$\begin{cases} \max\ y_1(x_1, x_2, x_3) \\ \max\ y_2(x_1, x_2, x_3) \\ s.t. \begin{cases} 250r/\min \le x_1 \le 500r/\min \\ 14mm \le x_2 \le 20mm \\ 1kg/s \le x_3 \le 2kg/s \end{cases} \end{cases} \tag{16}$$

The optimal parameter combination of the machine is as follows: the output speed of the motor is 443.77 r/min, the diameter of the screen is 14mm, the feeding amount is 1.27kg/s, the predicted productivity is 5078.28kg/h, and the silk rate is 94.93%.

In order to verify the reliability of the optimization results, the output speed of the motor was rounded to 445r/min, the feed volume was rounded to 1.3kg/s, and the screen diameter was selected to 14mm. The optimization results were verified. Each group of tests was repeated five times, and the average value of the five test results was calculated as the actual value of the evaluation index under this condition. The measured productivity is 5065.98kg/h, the silk ratio is 94.87%. The relative errors with the optimization results are 0.24% and 0.06%, respectively, indicating that the established mathematical model and the optimization results are accurate and reliable, and the kneading machine has good working performance.

CONCLUSIONS

(1) The cutting and crushing process of grass crusher was analyzed theoretically, and the key components such as cutting knife, hammer blade and serrated knife were designed. The modal analysis of cutting rotor and crushing rotor was carried out using ANSYS Workbench software, and the first 6 natural frequencies and corresponding vibration modes were obtained. The vibration mode of each order is analyzed in detail to avoid the damage of the whole machine due to the resonance phenomenon in the working process.

(2) Aiming at the simultaneous maximization of productivity and silking rate, the output speed, screen diameter and feeding amount of the motor were optimized by multi-objective solution, and the optimal parameter combination was obtained as follows: output speed of the motor was 443.77 r/min, screen diameter was 14 mm and feeding amount was 1.27 kg/s. The verification test showed that the productivity was 5065.98kg/h and the silking rate was 94.87%, which met the requirements of crushing alfalfa with high water content.

ACKNOWLEDGEMENT

This work was supported by Heilongjiang Bayi Agricultural University Graduate Innovative Research Project (YJSCX2023-Z02).

REFERENCES

[1] Bao, L., Li, Z., & Dongxing, Z. (2011). Force and motion states of hammer mill at unloaded running (锤片式粉碎机空载运行中锤片的受力及运动状态) [J]. *Transactions of the Chinese Society of Agricultural Engineering*, Vol.27, Issue 7, pp. 123-128. Henan/China.

[2] Decheng, W., Changbin, H., Hongjian, W., Yong, Y., & Guanghui, W. (2017). Review of Alfalfa Full-mechanized Production Technology. *Transactions of the Chinese Society for Agricultural Machinery*, Vol. 48, Issue 8, pp. 1-25. Beijing/China.

[3] Defu, W., Mo, W., & Liqiao, L. (2017). Mechanism Analysis and Parameter Optimization of Hammer Mill for Corn Stalk (锤片式粉碎机粉碎玉米秸秆机理分析与参数优化) [J]. *Transactions of the Chinese Society for Agricultural Machinery*, Vol.48, pp. 165-171.Heilongjiang / China.

[4] Guoqiang, F., Zhongyu, W., Baoxing, W., Jinxing, W.,Heyin, D., & Jian, H. (2021). Design and Experiment of Rotary Feed Tube Hammer Grinder (旋筒供料锤式饲草粉碎机设计与试验). *Transactions of the Chinese Society for Agricultural Machinery*, Vol. 52, Issue 12, pp.43-53. Shandong / China.

[5] Haijun, Z., Yi, Q. & Haiqing, T. (2024). Design and Experimental Optimization of V-shaped Hammer for Hammer Mill. *INMATEH-Agricultural Engineering*, Vol. 73, Issue 2, pp.191-200.Zhengjiang/China.

[6] Kun, W., & Yuepeng, S. (2022). Research Progress Analysis of Crop Stalk Cutting Theory and Method (农作物茎秆切割理论与方法研究进展分析) [J]. *Transactions of the Chinese Society for Agricultural Machinery*, (in Chinese). Vol.53, pp. 1-20. Shandong / China.

[7] Mei, F., Zhihong, Y., Wenjie, Z., Weifeng, L., Zhenjiang, B., & Jinbao, S. (2021). Analysis and experiments of the movement process for the shredded material of disc knife chaff cutter (盘刀式铡草机粉碎物料运动过程分析与试验). *Transactions of the Chinese Society of Agricultural Engineering*, Vol. 37, Issue 7, pp.76-84. Inner Mongolia/China.

[8] Qian, M., Fei, L., & Manquan. Z. (2016). Working mechanism and structure optimization of hammer of rubbing machine(揉碎机揉碎机理分析及锤片结构优化). *Transactions of the Chinese Society of Agricultural Engineering*, Vol. 32, Issue z2, pp. 7-15. Inner Mongolia/China.

[9] Songyi, L. (2019). *Design and Performance Test of Corn Straw Crushing Device (玉米秸秆揉碎装置设计与性能试验研究)*. Hohhot: Inner Mongolia Agricultural University. Inner Mongolia/China.

[10] Tao, C., Shujuan,Y., Yifei, L., Guixiang, T., Shanmin. Q. (2023). Establishment of Discrete Element Model and Parameter Calibration of Alfalfa Stem in Budding Stage (苜蓿现蕾期茎秆离散元模型建立与参数标定). *Transactions of the Chinese Society for Agricultural Machinery*, Vol. 54(5), pp.91-100. Heilongjiang/China.

[11] Tiejun, W., Tieliang, W., Hongguang, C., Yuanjuan, G., Subo, T., & Ruili W. (2021). Design and Experiment of Adjustable Feeding Straw Bale-breaking and Rubbing Filament Machine (喂入调节式秸秆破包揉丝机设计与试验). *Transactions of the Chinese Society for Agricultural Machinery*, Vol. 52(6), Issue 6, pp.148-158. Liaoning/China.

[12] Wei Z. (2016). *Design and performance test of 9RS-3 straw kneader (9RS-3 型秸秆揉丝机的设计与性能试验)*. Jinzhong: Shanxi Agricultural University.Shanxi/China.

[13] Weigang, L. (2019). *Analysis of straw crushing characteristics and optimization of crushing equipment structure*. Guiyang: Guizhou University. Guizhou/China.

[14] Xiaolong, H.,Yong, Y., & Decheng, W. (2021). Optimization Design and Experiment on Small Cutting and Beating Machine of King Grass (小型组合式王草铡切打浆机优化设计与试验). Transactions of the Chinese Society for Agricultural Machinery, Vol. 52, Issue 3 pp. 117-126.Beijing/China.

[15] Yajun, J., Yitao, L., & Qingxi, L. (2019). Design and Experiment on Cylinder-type Chopping Device of Harvester for Fodder Rapeseed in Winter and Spring (冬春鲜喂饲用油菜收获机滚刀式切碎装置设计与试验). *Transactions of the Chinese Society for Agricultural Machinery*, Vol. 50(2), pp.102-111. Hubei/China.

[16] Yong, Y., Hongda, W., Xiaolong, H., Decheng, W., Chenchen, K., & Bingnan. Y. (2021). Design and Experiment of Roller Crushing Device of King Grass Harvester (王草收获机滚筒破碎装置设计与试验). *Transactions of the Chinese Society for Agricultural Machinery*, Vol. 52(4), pp.134-142. Beijing/ China.

[17] Zhiqi, Z., Jin, H., Hongwen,L., Peisong, D.,Qingjie, W., & Xiangcai,Z. (2016). Design and Experiment of Straw-chopping Device with Chopping and Fixed Knife Supported Slide Cutting (动定刀支撑滑切式秸秆粉碎装置设计与试验). *Transactions of the Chinese Society for Agricultural Machinery*, Vol. 47, Issue s1, pp.108-116. Beijing/China.